Boundary-Layer Meteorol (2007) 123:29–54
DOI 10.1007/s10546-006-9139-4

ORIGINAL PAPER

The energy balance experiment EBEX-2000. Part II: Intercomparison of eddy-covariance sensors and post-field data processing methods

Matthias Mauder · Steven P. Oncley · Roland Vogt · Tamas Weidinger · Luis Ribeiro · Christian Bernhofer · Thomas Foken · Wim Kohsiek · Henk A. R. De Bruin · Heping Liu

Received: 19 December 2005 / Accepted: 16 October 2006 / Published online: 30 November 2006

Abstract The eddy-covariance method is the primary way of measuring turbulent fluxes directly. Many investigators have found that these flux measurements often

The National Center for Atmospheric Research is supported by the National Science Foundation.

M. Mauder (✉)
Department of Micrometeorology, University of Bayreuth, 95440 Bayreuth, Germany
Present address: Agriculture and Agri-Food Canada, Ottawa, Canada
e-mail: matthias.mauder@uni-bayreuth.de

S. P. Oncley
National Center for Atmospheric Research Boulder, CO, USA

R. Vogt
University of Basel, Basel, Switzerland

T. Weidinger
Eötvös Loránd University, Budapest, Hungary

L. Ribeiro
Bragança Polytechnic Institute, Bragança, Portugal

C. Bernhofer
Dresden University of Technology, Dresden, Germany

T. Foken
University of Bayreuth, Bayreuth, Germany

W. Kohsiek
KNMI Royal Dutch Meteorological Institute, Utrecht, The Netherlands

H. A. R. De Bruin
Wageningen University, Wageningen, The Netherlands

H. Liu
City University of Hong Kong, Kowloon, Hong Kong SAR, P. R. China
Present address: Jackson State University, Jackson, MS, USA

do not satisfy a fundamental criterion—closure of the surface energy balance. This study investigates to what extent the eddy-covariance measurement technology can be made responsible for this deficiency, in particular the effects of instrumentation or of the post-field data processing. Therefore, current eddy-covariance sensors and several post-field data processing methods were compared. The differences in methodology resulted in deviations of 10% for the sensible heat flux and of 15% for the latent heat flux for an averaging time of 30 min. These disparities were mostly due to different sensor separation corrections and a linear detrending of the data. The impact of different instrumentation on the resulting heat flux estimates was significantly higher. Large deviations from the reference system of up to 50% were found for some sensor combinations. However, very good measurement quality was found for a CSAT3 sonic together with a KH20 krypton hygrometer and also for a UW sonic together with a KH20. If these systems are well calibrated and maintained, an accuracy of better than 5% can be achieved for 30-min values of sensible and latent heat flux measurements. The results from the sonic anemometers Gill Solent-HS, ATI-K, Metek USA-1, and R.M. Young 81000 showed more or less larger deviations from the reference system. The LI-COR LI-7500 open-path H_2O/CO_2 gas analyser in the test was one of the first serial numbers of this sensor type and had technical problems regarding direct solar radiation sensitivity and signal delay. These problems are known by the manufacturer and improvements of the sensor have since been made.

Keywords EBEX-2000 · Eddy covariance · Energy balance closure · Quality control · Sensor intercomparison · Turbulent fluxes

1 Introduction

In 1994, a workshop of the European Geophysical Society in Grenoble (Foken and Oncley 1995), developed the idea for the energy balance experiment EBEX-2000. This experiment was designed to investigate potential reasons for the non-closure of surface energy balance measurements (Oncley et al. 2002, 2006); see also Laubach and Teichmann (1996), Foken (1998), Aubinet et al. (2000), Wilson et al. (2002), Culf et al. (2004). One concern of the Grenoble workshop was that different types of sonic anemometers showed significant differences in their characteristics and whether eddy-covariance sensors produce acceptable data. In order to address this issue a field comparison of most recently available eddy-covariance sensors was a main focus of EBEX-2000.

At the beginning of modern turbulence measurements in the 1960s, sonic comparison experiments were common, because the developers of the sensors often were participants of micrometeorological field experiments. Results from four such experiments are published, including interesting surface-layer studies. The first experiment was carried out in 1968 near Vancouver, Canada, over the ocean (Miyake et al. 1971), followed by one over steppe country at Tsimlyansk, Russia in 1970 (Tsvang et al. 1973). Additional experiments were carried out in 1976 in Conargo, Australia (Dyer 1981; Dyer et al. 1982) and in 1981 again in Tsimlyansk (Tsvang et al. 1985). In these early intercomparison experiments mostly prototype instrumentation was tested. During the last 10–15 years several commercially built sonic anemometers have become available, but most of the sonic anemometer comparisons are only available in the grey literature. Many recent micrometeorological experiments have still included a comparison phase, though most of these sonic intercomparisons are unpublished reports

(Table 1). Fast-response hygrometers should also be compared, in order to determine the accuracy of latent heat flux measurements.

A second major question in the investigation of the non-closure of energy balance measurements is whether typical differences in post-field data processing methods have a significant impact on eddy-covariance flux estimates. Most of the processing steps and flux corrections are well described in the literature (e.g. Webb et al. 1980; Schotanus et al. 1983; Moore 1986; Højstrup 1993; Tanner et al. 1993; Wilczak et al. 2001). Temperature and humidity effects, which are discussed by Högström and Smedman (2004) as a source of error for sonic anemometer measurements, can be avoided by the application of these correction algorithms. However, errors in the resulting turbulent heat fluxes can also occur due to differences in the selection and in the order of the processing steps, and because of the use of oversimplified or modified algorithms and different values for physical constants. In order to address these methodological problems a comparison of several post-field data processing methods was carried out.

2 Comparison of post-field data processing methods

Each of the groups participating in EBEX-2000 processed two days of data from one eddy-covariance system that was operated by the U.S. National Center for Atmospheric Research NCAR during the EBEX-2000 experiment. The resulting turbulent flux estimates were compared on the basis of a 30-min averaging time. Since each group started with identical time series, we expected the computed fluxes to be quite similar. Table 2 gives an overview of the features implemented in the post-field data processing methods of the EBEX-2000 participants. Certainly, progress has been made in the data processing methods since then, particularly in light of this investigation. However, the results of this comparison can be used to demonstrate typical differences. For this reason, the processing methods are made anonymous and labelled A–E.

In many of the post-field data processing methods a spike detection algorithm (e.g. Højstrup 1993) is implemented. From the despiked time series covariances can be calculated after either block averaging or linear detrending. Coordinate systems can be transformed either by using two- or three-dimensional rotation (Kaimal and Finnigan 1994) or according to the planar fit method (Wilczak et al. 2001). If no additional fast response thermometer is available, the vertical sonic temperature flux (buoyancy flux) has to be converted into the sensible heat flux either according to the relations of Schotanus et al. (1983) or Liu et al. (2001). Krypton hygrometers have a cross sensitivity to oxygen, which can be corrected (Tanner et al. 1993; van Dijk et al. 2003). Spectral loss due to pathlength averaging, sensor separation or dynamic frequency response can be corrected as proposed by Moore (1986) or Horst (2000). When measuring volume-related fluxes of air constituents such as water vapour, the so called WPL correction has to be applied (Webb et al. 1980) in order to compensate for density fluctuations and a positive vertical mass flow. Some post-field data processing methods include the correction of Brook (1978). However, this correction should not be applied because of incorrect assumptions (Webb 1982), such as the formulation of the sensible heat flux, which lead to different opinions about which terms are negligible or not.

Finally, it makes a difference if physical "constants" such as the latent heat of vaporisation λ or the specific heat capacity of the air at constant pressure c_p are assumed

Table 1 List of sonic anemometers types operated in selected intercomparison experiments; the sonic type used as reference is identified

Sensor	LINEX-96/2 (Foken et al. 1997)	LITFASS-98 (Beyrich et al. 2002)	MAP-Riviera (Christen et al. 2000)	VOITEX-99 (Foken 1999)	UBL/CLU (Mestayer et al. 2005)	EBEX-2000 (this paper)
Campbell CSAT 3	X	X	X (ref.)	X (ref.)	X	X (ref.)
Kaijo-Denki 310/A	X (ref.)	X (ref.)	–	–	–	–
Kaijo-Denki 310/B	–	X	–	–	–	–
Kaijo-Denki TR90-AH	–	–	–	–	–	X
Solent-HS	–	–	X	–	–	X
Solent R2/R3	X	–	X	X	X	–
Metek USA–1	X	–	X	X	X	X
R. M. Young 81000	–	–	–	X	X	X
ATI K Probe	–	–	–	–	–	X
UW Sonic	–	–	–	–	–	X

LINEX-96/2: Lindenberg Experiment; LITFASS-98: Lindenberg Inhomogeneous Terrain—Fluxes between Atmosphere and Surface: a long term Study; MAP-Riviera-99: Mesoscale Alpine Programme in the Riviera valley; VOITEX-99: Voitsumra Experiment; EBEX-2000: Energy Balance Experiment

Table 2 Data processing steps and physical constants in the software packages of the EBEX-2000 participants as of 2002

Step	A	B	C	D	E	TK2
1	Despike	Despike	(Despike)	Linear Detrend.	Linear Detrend.	Despike
2	Linear Detrend. Block Average	Linear Detrend.	Block Average	3D Rot. $\overline{w}=0$; $\overline{v}=0$; $\overline{v'w'}=0$	3D Rot. $\overline{w}=0$; $\overline{v}=0$; $\overline{v'w'}=0$	
3	2D Rot. $\overline{w}=0$; $\overline{v}=0$	3D Rot. $\overline{w}=0$; $\overline{v}=0$; $\overline{v'w'}=0$	Planar fit + $\overline{v}=0$	Moore	$t_c \rightarrow t$, Schotanus et al.	Crosswind, Liu et al.
4	$t_c \rightarrow t$, Schotanus et al.	$t_c \rightarrow t$, Schotanus et al.	$t_c \rightarrow t$, Schotanus et al.; Oxygen; WPL	$t_c \rightarrow t$, Schotanus et al.	Oxygen	Planar fit + $\overline{v}=0$
5	Moore	WPL	Brook	WPL	WPL	Oxygen
6	WPL	Moore			Moore	Moore
7		Brook				$t_c \rightarrow t$, Schotanus et al.
8						WPL
9						iteration of interdependent processing steps
10						QA/QC, Foken and Wichura
Constants	$\lambda = \text{const}$; $c_p = \text{const}$	$\lambda(T)$; $c_p(c_{p,\text{dry}}; q)$;	$\lambda(T)$; $c_p(c_{p,\text{dry}}; q)$	$\lambda = \text{const}$; $c_p = \text{const}$	$\lambda = \text{const}$; $c_p = \text{const}$	$\lambda(T)$; $c_p(c_{p,\text{dry}}; q)$

TK2 was used as reference for the eddy-covariance intercomparison. The other post-field data processing methods are made anonymous and labelled A, B, C, D and E

Moore: spectral correction according to Moore (1986); WPL: correction for density effects by Webb et al. (1980); Brook: correction for water vapour fluctuations by Brook (1978); Oxygen: correction for oxygen cross sensitivity of krypton hygrometers (Tanner et al. 1993; van Dijk et al. 2003); Schotanus et al.: conversion of buoyancy flux into sensible heat flux according to Schotanus et al. (1983); Liu et al.: crosswind correction sensible heat flux according to Liu et al. (2001)

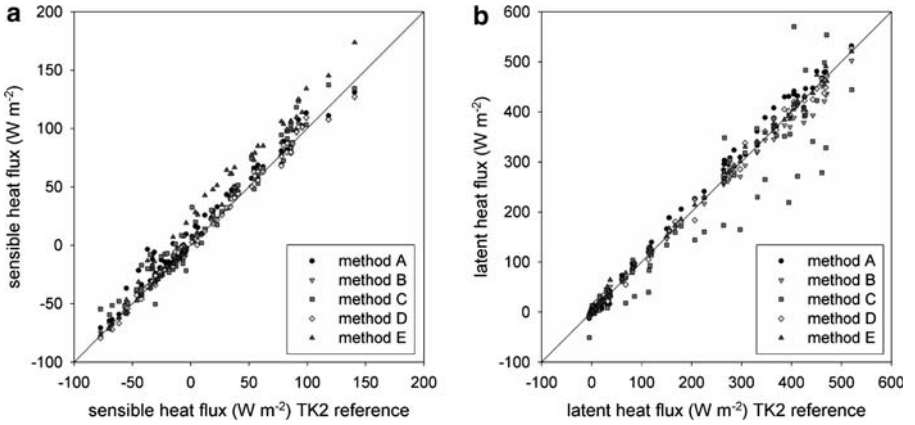

Fig. 1 Results for turbulent fluxes calculated from the same time series (measured with the NCAR system at EBEX-2000 site 8, 1700 UTC, August 9 2000 to 1700 UTC, August 11 2000) using different post-field data processing methods of the EBEX-2000 participants; sensible heat flux on the left (**a**), latent heat flux on the right (**b**). Results of methods A,B,C,D and E are plotted against reference software TK2 (Mauder and Foken 2004)

to be constant or if their dependences on temperature and moisture are taken into account. Tools proposed by Foken and Wichura (1996) can be applied for the quality assessment and quality control of eddy-covariance measurements.

In general, differences between the tested post-field data processing methods of up to 2% were seen in the momentum flux (not shown) of up to 10% in the sensible heat flux, and of up to 15% in the latent heat flux (see Fig. 1). About 10% of the difference in latent heat flux values was due to one group (C) not correcting properly for the spatial displacement of about 0.3 m between the sonic anemometer and the hygrometer. A second important aspect was whether linear detrending was applied to the time series, because it acts as a high-pass filter and is therefore not appropriate (Finnigan et al. 2003). Finally, the procedure used to apply the Schotanus correction for the sensible heat flux can have a significant impact. This can be especially seen for method E (Fig. 1a). The sensible heat fluxes obtained from this method are approximately 10% larger than the reference because the Schotanus correction was not applied properly.

The method of anemometer coordinate rotation and implementations of the oxygen, WPL and other corrections appear to have similar effects on the computed fluxes for all processing methods. Part of the scatter in Fig. 1a,b can be attributed to the use of different definitions for physical constants. Another part of this scatter is due to a different order or formulation of processing steps. As a result of this methodology comparison, we agreed to uniformly calculate all EBEX-2000 sensor intercomparison data with one software package (see Sect. 5.1).

3 Comparison of eddy-covariance sensors

3.1 Sonic anemometers

Several new models of sonic anemometers were used during EBEX-2000 to determine turbulent fluctuations of wind velocity and temperature. Table 3 gives their primary characteristics. Representative instruments of each of these types were tested during

Table 3 A summary of the sonic anemometer array characteristics

Array	Pathlength l (mm)	Transducer diameter d (mm)	l/d	Orthogonal paths	Intersecting paths
CSAT 3,Campbell Sci.	120	6.4	19	N	Y
UW, NCAR	200	10	20	N	Y
Solent-HS, Gill Instr.	150	11	14	N	Y
K-Probe, ATI	150	10	15	Y	N
TR90-AH, Kaijo Denki	50	5.5	9	Y	Partially
USA-1, Metek	175	20	9	N	N
Model 81000, R.M. Young	150	13.8	11	N	Y

side-by-side intercomparisons. Photographs of the sensors that were used during the EBEX-2000 field comparison are provided in Fig. 3.

CSAT3, Campbell Scientific: Most of the participants in EBEX-2000 used Campbell Scientific sonic anemometers (CSAT3), and three of these were deployed during the intercomparison period in the beginning of EBEX-2000. The CSAT3 has three intersecting, non-orthogonal, acoustic paths tilted 60 degrees from the horizontal plane. The pathlength l is 120 mm and transducers are 6.4 mm in diameter d, so $l/d \approx 19$. The transducers are supported by arms on the top and bottom that meet at the back of the array. Thus, airflow should be unobstructed except for winds coming from the back of the array. With these characteristics, the data are considered free from flow distortion (Wyngaard and Zhang 1985) if winds from within 30 degrees of the back of the array are discarded. The acoustic temperature data are internally corrected for crosswind contamination.

UW, NCAR: This array was initially built at the University of Washington (Zhang et al. 1986) and has been duplicated by NCAR, now based on the electronics by ATI (see below). Its geometry of three intersecting paths supported from the back was a model for the CSAT3 design and its thinner construction should result in even less distortion of the flow. With $l/d = 20$ and only one, thin, structural element, no flow distortion correction is used, with data from within 20 degrees of the back discarded. Crosswind corrections are applied in post processing.

Solent HS, Gill Instruments: Again, this array has three non-orthogonal paths, though the transducers are arranged in such a way that this array is symmetric to rotation around the longitudinal axis, but not symmetric to flipping about the longitudinal-vertical plane. With $l/d \approx 14$, a correction for distortion of the flow by the transducers is necessary, even though the transducer orientation is similar to the UW. This is done internally via a look-up table in azimuth and a generic correction in the vertical. For the EBEX-2000 intercomparison study, this correction was turned off, as we intended to examine the sensors' real response. Moreover, studies by Högström and Smedman (2004) showed that these wind-tunnel-based corrections cannot be simply transferred to the atmospheric turbulent flow. Again, the sonic temperature is internally corrected for crosswind contamination.

TR90-AH, Kaijo-Denki: The Kaijo-Denki TR90-AH has three orthogonal paths. Each horizontal path intersects the vertical path, but does not intersect the other horizontal path. The transducers are supported by independent arms that meet in the back of the array, so the flow is completely unobstructed only for a 90 degree sector of wind

directions. Due to its filigree structure, the TR90-AH can measure small eddies close to the ground.

K probe, ATI: The K probe has three orthogonal, completely non-intersecting paths. Kaimal et al. (1990) describe this array as having flow distortion that can be corrected by considering only the effects of a single path. The path velocity is assumed to be attenuated by a factor $1 - f \cos\theta$ where θ is the angle between the wind and along-path vectors and f is an empirically determined flow distortion correction coefficient (cf. Wyngaard and Zhang 1985). The acoustic temperature is derived only from the vertical path.

USA-1, Metek: The Metek USA-1 has a unique geometry with three non-orthogonal non-intersecting paths supported by a central post. Although the wake shed by this post is always sampled by one of the paths, the affected path is always nearly perpendicular to the wind and thus observing nearly zero velocity. Therefore, the magnitude of the wake correction is expected to be relatively small. Only the relatively large transducer heads probably cause some transducer-shadow effects. Metek provides two options for a flow distortion correction, which can be performed internally. The first uses azimuth dependent correction equations for the three wind components (head correction HC1), the second is based on a three-dimensional look-up table (head correction HC4). HC1 has been applied when analysing the USA-1 data for this intercomparison experiment.

Model 81000, R.M. Young: The R.M. Young sonic uses transducers that are nearly identical to the Solent-HS; however, they are supported by three vertical posts and the electronics are in a tube just below the array. The anemometer probably requires a generic correction for the influence of wakes from these posts and from the transducers, but this is not documented. The tube that supports the transducers array probably also influences the flow inside the measurement volume. A crosswind correction is applied internally.

3.2 Fast-response hygrometers

A special focus of the EBEX-2000 intercomparison activities was on the measurement uncertainties of latent heat flux using fast-response hygrometers. Most of the instruments deployed were krypton hygrometers, and so this part of the study mainly investigates differences between different sensors of this single sensor type. In addition, a comparison was made using a LI-7500 open path infrared gas analyser at site 7.

KH20, Campbell Scientific: The KH20 krypton hygrometer measures the absorption of ultraviolet light emitted by a krypton gas discharge lamp at a major line at 123.58 nm and a minor line at 116.49 nm (Tanner and Campbell 1985). This light is mainly absorbed by water molecules in the measuring path but also to a minor degree by oxygen in the air. In order to obtain the water content of the measuring volume, one has to correct for the cross sensitivity to oxygen (Tanner et al. 1993; van Dijk et al. 2003). Due to the relatively strong absorption at this wavelength, this instrument is highly sensitive so it is appropriate for deployment even in dry conditions, e.g. deserts, or at low temperatures. Its pathlength is typically about 10 mm.

There are restrictions to the use of the KH20 according to the manufacturers' instructions. It is supposed to be deployed for short, attended studies only, as some components must be protected from precipitation and condensing humidity. It does

not measure absolute concentrations. Only measurements of fluctuations are possible. Routine maintenance is required to keep source and detector windows free of scale, which is caused by a disassociation of atmospheric constituents by the ultraviolet photons (Tanner and Campbell 1985). The rate of scaling is a function of the atmospheric humidity, and in high humidity environments, scaling can occur within a few hours, attenuating the signal and causing shifts in the calibration curve. However, in theory this effect should only cause an offset of the humidity signal and not a change in the slope of the calibration function. Therefore, its impact on the results for variances and covariances over a 30-min interval should be negligible. Thus, water vapour fluctuation measurements can still be made with this hygrometer. The effects of scaling can be reversed by wiping the windows with a moist swab.

LI-7500, LI-COR: The open path infrared gas analyser LI-7500 from LI-COR has a fixed pathlength of 125 mm, which is one order of magnitude larger than the KH20. Therefore, it cannot resolve very small eddies close to the ground. The windows are sapphire and quite robust. In contrast to the KH20, the LI-7500 is capable of measuring both water vapour and CO_2 concentrations. Infrared light of non-absorbing wavelengths 3.95 and 2.40 μm is used as a reference for attenuation corrections. CO_2 and H_2O are measured through absorption at wavelengths centred at 4.26 and 2.59 μm. Internal digital signal processing applies antialiasing filtering.

Early serial numbers of this sensor suffered from two major problems, which have now been resolved by the manufacturer. First, the solar-radiation error: the LI-7500's detector is sensitive not only to infrared light, which is emitted by the instrument itself and absorbed by molecules in the measuring path, but also to sunlight. For clear skies with constant irradiance this effect only causes a bias in the LI-7500 signals. However, scattered clouds or changing humidity is reflected in additional variance in the humidity and CO_2 data series. Serial numbers prior to 75H-0283 were affected by this unwanted sensitivity to direct sunlight.

Secondly, a delay time error was published by LI-COR in July 2003. The internal signal processing causes some time delay, which can be controlled via software by the user. The software version 2 was faulty because the delay time setting in the software did not correspond with the real delay time of the signal. Turbulent fluxes of H_2O and CO_2 would be underestimated if a fixed wrong time lag for the calculation of covariances was used. During EBEX-2000 one of the first LI-7500 sensors (SN# 75H-0006) was used, so both errors are potentially relevant for us. The first error should have a small effect since skies during EBEX-2000 were usually cloud free. The second error was compensated for during the data post-processing by the application of a cross correlation analysis to find the maximum covariance between H_2O and the vertical wind velocity for each averaging interval. This approach implies also a frequency response correction for longitudinal spatial separation between the sonic and the fast-response humidity sensor (Moore 1986).

4 Experimental set-up

The EBEX-2000 experiment took place in the San Joaquin Valley of California on an irrigated cotton field of 1.30 km^2 size near Lemoore, CA (Oncley et al. 2002). The canopy height varied between 0.80 m and 0.95 m. The measurement systems were operated from July 20 to August 24, 2000, during which period the cotton plants grew

rapidly. Consequently, evaporation was the dominant process of energy transfer into the air. This is indicated by typical Bowen ratios in the order of 0.1–0.2 at noon. The weather was characterised by clear skies, and air temperatures typically ranged from 15°C during the night to maxima up to 35°C during daytime. The water vapour pressure over the cotton field showed quite strong variations and ranged from 10 hPa to 25 hPa. The experimental set-up comprised ten sites distributed over the field, each equipped with eddy-covariance systems, soil and radiation sensors.

EBEX-2000 featured many side-by-side eddy-covariance sensor intercomparisons. For the most part, sensors were placed on adjacent towers to avoid flow interference, the typical distance between the towers being 6 m. Since the EBEX-2000 field site was a relatively uniform crop of cotton for about 1 km upwind, and had extremely flat topography for at least 100 km upwind (Oncley et al. 2002), we assume that the air flow had the same statistics at each sensor location. The wind direction is channelled by larger-scale topography in this location and was from the north-north-west for the vast majority of data collected. The towers were aligned perpendicular to this direction to reduce flow interference.

The first 10 days of the field campaign were reserved for the eddy-covariance sensor intercomparison. The sensors were deployed at site 8, as described by Oncley et al. (2007), in the middle of the downwind portion of the field, and were mounted at a height of 4.7 m above ground level. This measuring height was well within the internal boundary layer for this field. According to Jegede and Foken (1999) the internal boundary layer was more than 9 m high at that position, assuming winds from the north-north-west. Fig. 2 shows the array of towers.

During the remainder of the experiment, several other pair-wise comparisons were possible with sensor types that, for some reason, could not be deployed in the main intercomparison. This was the case at site 7, where four different eddy-covariance systems were operated on different towers in a line of east-west orientation.

Figure 3 shows each of the sensors that participated in the intercomparison array. These sonics were deployed by groups from the following institutions: National Center for Atmospheric Research (NCAR), University of Basel (UBS), Royal Dutch Meteorological Institute (KNMI), Wageningen University (WU), City University of

Fig. 2 View of the intercomparison array from the north-west. Note the overall uniformity of the terrain; the site 8 profile towers to the left of the intercomparison towers, and the site 9 profile towers in the background on the right

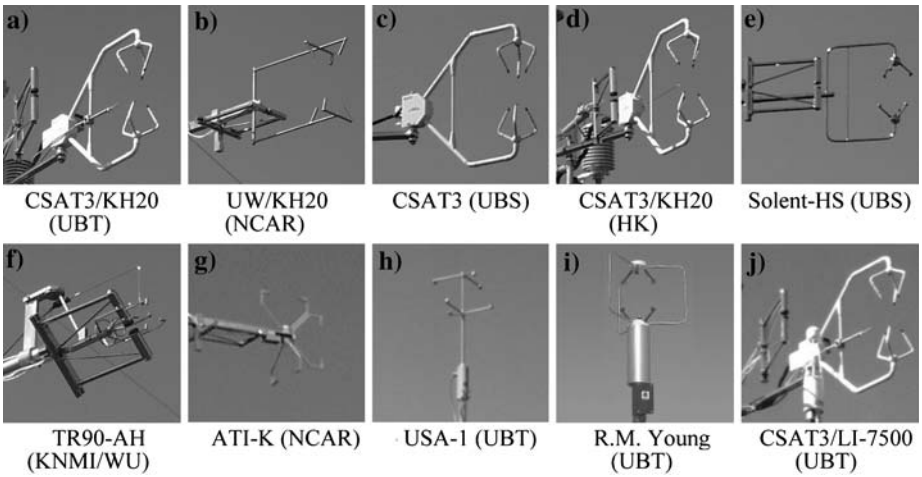

Fig. 3 Representative eddy-covariance sensors used during EBEX-2000. The sensors during the main intercomparison at site 8 are: **a, b, c, d, e, f**, and **g**. Side-by-side comparison at site 7: **h, i, j**. Note the deployment of krypton hygrometers with all of these except **c, h, i**

Hong Kong (HK), and University of Bayreuth (UBT). All instruments were oriented into the prevailing wind direction. Hygrometers were located downwind of the sonic arrays, in order to minimise flow distortion. Only the KH20, which was deployed together with the Kaijo-Denki from KNMI/WU, was located very close to the sonic (see Fig. 3f), in order to minimise spectral loss due to sensor separation. This was especially important for this system, because it later was deployed close to the ground, where turbulence spectra are shifted to smaller eddy sizes in general.

The data from all fast-response sensors were sampled at a frequency of 20 Hz. During the main sensor intercomparison at site 8 all high-frequency data were collected and stored using NCAR's data acquisition system (Businger et al. 1990). During the intercomparison at site 7, the data from NCAR's ATI-K, UBT's CSAT3/KH20, the USA-1 and the R.M. Young were also recorded via NCAR's data acquisition system. The data from the LI-7500 gas analyser were recorded separately on a Campbell CR23X data logger. These data were synchronised with the CSAT3/KH20 system by applying a cross correlation analysis as described in Sect. 3.2. All krypton hygrometers deployed by NCAR were calibrated in the laboratory a few weeks before the experiment. All other KH20s were calibrated the day after the EBEX-2000 measurement period. For the LI-7500, the manufacturer's calibration was applied.

5 Data preparation for the sensor intercomparison

5.1 Post-field data processing of the turbulence measurements

All turbulence data have been processed in the same way. The calculation was done in two steps. First, the raw turbulence statistics were calculated after a de-spiking procedure with the NCAR software package (Oncley et al. 2007). Flux corrections and quality checks were applied to these data using the TK2 software package of the

University of Bayreuth (Mauder and Foken 2004), which was developed according to the guidelines composed by Lee et al. (2004). The processing steps were performed in the order as they are presented in Table 2. Furthermore, all corrections were iterated because of their interdependence. The crosswind correction was only applied if not already implemented in the sonic software (see Sect. 3).

5.2 Statistical analysis of the intercomparison

In any comparison study it is necessary to choose a reference sensor. We used the Bayreuth CSAT3, which was deployed together with a KH20 (see Fig. 3a), since its characteristics are well described in earlier intercomparisons (Foken et al. 1997; Foken 1999; Beyrich et al. 2002). It was deployed in the middle of the intercomparison array and had good data recovery; furthermore, this sensor was at site 7 during the operational period of EBEX-2000. There, the remainder of the anemometers that were not available during the intercomparison period could be compared to this reference. We had to make one exception regarding the reference instrument, because the ATI-K probe at site 8 was not deployed at the same time as the Bayreuth CSAT3. Here the NCAR UW served as a reference instrument, because it showed the best overall agreement with the Bayreuth CSAT3.

All turbulence statistics presented herein are based on 30-min block averages. Tables 4 to 10 summarise the statistical analyses of the sensor comparisons. The results of the regression analysis are given as the absolute value of the regression equation a (intercept), the regression coefficient b or slope of the regression line, and the coefficient of determination R^2. Additionally, the root-mean-square deviation $rmsd$, also called the comparability, and the bias d (ISO 1993) are listed:

$$d = \frac{1}{n} \sum \left(x_{a,i} - x_{b,i} \right), \tag{1}$$

$$rmsd = \sqrt{\frac{1}{n} \sum \left(x_{a,i} - x_{b,i} \right)^2}, \tag{2}$$

where n is the number of observations, $x_{a,i}$ is ith observation of the sensor being evaluated, $x_{b,i}$ is ith observation of the reference instrument.

These comparisons are made for several quantities that can be measured by eddy-covariance sensors: averages of wind speed, variances of vertical wind, sonic temperature, and humidity, as well as covariances, particularly friction velocity and the turbulent fluxes of sensible and latent heat.

5.3 Data selection

For the NCAR UW sonic, the sector between 250° and 270° seems to be distorted. This becomes obvious in increased variances in all three wind components. A neighbouring tower carrying an ATI-K probe probably acted as obstacle for the air flow coming from this wind direction. Therefore, this sector was excluded from the intercomparison. At site 7, on some of the nights we found very large differences between fluxes measured by the different sensors. Normalized standard deviations, also known as integral turbulence characteristics (e.g. Foken et al. 1991; Foken and Wichura 1996; Thomas and Foken 2002; Foken et al. 2004; Mölder et al. 2004), were used to detect such periods. Low values of integral turbulence characteristics indicate that turbulence

is not well developed. Therefore, all data with $\sigma_w/u_* < 1.00$ were discarded, with σ_w being the standard deviation of the vertical wind velocity w, and u_* being the friction velocity, where

$$u_* = \left(\overline{u'w'}^2 + \overline{v'w'}^2\right)^{1/4}. \quad (3)$$

Under such conditions one cannot assume that neighbouring sensors are really measuring the same statistics. In contrast, data that failed the steady state test were not excluded, because in this case neighbouring eddy-covariance systems still should measure the same turbulent properties.

6 Results of the sensor intercomparison

6.1 Horizontal wind speed

The first parameter to be compared is the horizontal wind speed $\overline{u}$ measured by the different sonic anemometers. This $\overline{u}$ value is the average of the longitudinal horizontal wind component after a planar fit coordinate transformation and rotation into the mean wind direction. Table 4 shows the results of the statistical analysis. The best agreement can be found for the NCAR UW. The other two CSATs from the Universities of Basel and Hong Kong measure similar wind speeds, too, as expected for instruments of the same type. The Solent-HS deviates further from the reference system. Systematic differences of more than 5% from the 1:1 line were found for the Kaijo-Denki TR90-AH, the USA-1, and the R.M. Young. The two ATI-K probes also overestimate the wind speed. The use of a flow distortion correction factor of $f = 0.16$ improves the results slightly compared to a factor $f = 0.20$.

6.2 Variance of vertical wind

Next, variances of the measured turbulent quantities are compared. Table 5 shows that the UW sonic and the two CSATs agree well with the reference measurement of the variance of the vertical wind component $\overline{w'w'}$ with $R^2 \geq 0.98$ and $0.99 \leq b \leq 1.02$.

Table 4 Comparison of the horizontal wind speed $\overline{u}$ measurements during EBEX-2000, using CSAT3 (UBT) as reference. Values causing concern are underlined

Sensor	Abs. value a ($\mathrm{m\,s^{-1}}$)	Regression coefficient b	R^2	Comparability $rmsd$ ($\mathrm{m\,s^{-1}}$)	Bias d ($\mathrm{m\,s^{-1}}$)
UW (NCAR)	−0.00	1.02	0.99	0.08	0.03
CSAT3 (UBS)	−0.01	1.03	0.99	0.09	−0.04
CSAT3 (HK)	−0.06	1.04	1.00	0.08	0.02
Solent-HS (UBS)	−0.09	1.05	0.98	0.11	−0.09
TR90-AH (KNMI/WU)	−0.17	0.96	0.96	0.30	−0.26
ATI-K (NCAR) S8[a] $f = 0.16$	−0.06	1.03	1.00	0.06	0.01
ATI-K (NCAR) S8[a] $f = 0.20$	−0.06	1.06	1.00	0.09	0.07
ATI-K (NCAR) S7	0.01	1.04	0.99	0.13	−0.07
USA-1 (UBT)	−0.12	1.06	0.97	0.19	0.03
R.M. Young (UBT)	0.17	0.92	0.98	0.10	0.01

[a] Here NCAR's UW served as reference instrument, since the Bayreuth CSAT3 was not deployed at the same time as the ATI-K probe at site 8

Table 5 Comparison of the vertical wind variance $\overline{w'w'}$ measurements during EBEX-2000, using CSAT3 (UBT) as reference. Values causing concern are underlined

Sensor	Abs. value a ($m^2\,s^{-2}$)	Regression coefficient b	R^2	Comparability $rmsd$ ($m^2\,s^{-2}$)	Bias d ($m^2\,s^{-2}$)
UW (NCAR)	0.000	0.99	0.98	0.010	−0.001
CSAT3 (UBS)	−0.000	0.99	0.99	0.007	−0.001
CSAT3 (HK)	−0.000	1.02	1.00	0.006	0.001
Solent-HS (UBS)	0.000	0.89	0.99	0.010	−0.006
TR90-AH (KNMI/WU)	−0.013	1.26	0.99	0.021	−0.014
ATI-K (NCAR) S8[a] $f = 0.16$	0.000	1.11	1.00	0.008	0.005
ATI-K (NCAR) S8[a] $f = 0.20$	0.000	1.11	1.00	0.009	0.005
ATI-K (NCAR) S7	−0.000	1.13	0.99	0.010	0.005
USA-1 (UBT)	0.000	0.93	0.99	0.009	−0.004
R.M. Young (UBT)	−0.000	1.06	0.98	0.007	0.003

[a] Here NCAR's UW served as reference instrument, since the Bayreuth CSAT3 was not deployed at the same time as the ATI-K probe at site 8

The Solent-HS is systematically low by approximately 10% because it was operated without the internal flow distortion correction, which would increase vertical wind velocities by a generic factor of 1.10. Thus, after the application of this correction it would agree quite well with the reference system. The Kaijo-Denki measurements are heavily distorted by the obstruction of the KH20, indicated by the largest values for comparability and bias of all instruments tested. The two ATI-K probes report $\overline{w'w'}$ larger by more than 10%, no matter which flow distortion correction factor is applied. Variances of the vertical wind measured by the Metek are systematically lower than the reference. Those measured by the R.M. Young are systematically overestimated.

6.3 Variance of sonic temperature

The accuracy of sonic temperature fluctuation measurements (given in Table 6) is crucial for the determination of the sensible heat flux. Again, the UW and the two CSATs show very good agreement with the reference system for the variance of the sonic anemometer $\overline{t_c't_c'}$. Although the wind measurements of the TR90-AH are disturbed, the sonic temperature measurements appear to be unaffected. The Solent-HS obviously has major problems with sonic temperature measurements, which result in large systematic deviations and considerable scatter. Both the USA-1 and the R.M. Young underestimate $\overline{t_c't_c'}$ systematically. The results of the site 8 ATI-K probe are in good agreement with the reference system, whereas the site 7 underestimates $\overline{t_c't_c'}$ slightly.

6.4 Variance of absolute humidity

For the variance of absolute humidity $\overline{\rho_v'\rho_v'}$, only the NCAR KH20, which was deployed with the UW sonic, shows satisfactory agreement with the reference system (Table 7), having the smallest values for comparability and bias of all the instruments tested. The comparability and bias of the KNMI/WU KH20 are slightly worse than those from UW/KH20 (NCAR), due to stronger overestimation of humidity fluctuations by this hygrometer. The second NCAR krypton hygrometer, which was deployed together with the ATI-K probe, also overestimates $\overline{\rho_v'\rho_v'}$. The humidity fluctuations measured by the KH20 from the University of Basel (UBS) have a strong negative

Table 6 Comparison of the sonic temperature variance $\overline{t_c' t_c'}$ measurements during EBEX-2000, using CSAT3 (UBT) as reference. Values causing concern are underlined

Sensor	Abs. value a (K^2)	Regression coefficient b	R^2	Comparability $rmsd$ (K^2)	Bias d (K^2)
UW (NCAR)	0.002	1.00	0.99	0.031	0.002
CSAT3 (UBS)	0.003	0.97	0.99	0.031	−0.004
CSAT3 (HK)	0.001	1.00	0.99	0.018	0.001
Solent-HS (UBS)	−0.018	1.45	0.92	0.174	0.080
TR90-AH (KNMI/WU)	0.000	1.00	0.98	0.034	−0.001
ATI-K (NCAR) S8[a]	0.003	0.98	1.00	0.024	−0.003
ATI-K (NCAR) S7	0.012	0.94	0.99	0.042	−0.005
USA-1 (UBT)	−0.003	0.86	0.98	0.060	−0.036
R.M. Young (UBT)	0.014	0.85	0.98	0.086	−0.036

[a] Here NCAR's UW served as reference instrument, since the Bayreuth CSAT3 was not deployed at the same time as the ATI-K probe at site 8. The flow distortion correction factor f is not relevant for sonic temperature measurements

Table 7 Comparison of absolute humidity variance $\overline{\rho_v' \rho_v'}$ measurements during EBEX-2000, using KH20 (UBT) as reference. Values causing concern are underlined

Sensor complex	Abs. value a (g^2m^{-6})	Regression coefficient b	R^2	Comparability $rmsd$ (g^2m^{-6})	Bias d (g^2m^{-6})
UW/KH20 (NCAR)	0.021	1.06	0.99	0.143	0.060
CSAT3/KH20 (HK)	0.021	0.30	0.97	0.621	0.353
Solent-HS/KH20 (UBS)	0.004	0.73	0.99	0.279	−0.166
TR90-AH/KH20 (KNMI/WU)	0.006	1.12	0.99	0.159	0.087
CSAT3/LI-7500 (UBT)	−0.013	1.50	0.99	0.943	0.505
ATI-K/KH20 (NCAR)	−0.014	1.17	0.98	0.354	0.148

bias and also show a low slope of the regression line. However, the scatter and the intercept are small. There is a major problem with the sensitivity of the Hong Kong KH20 (HK), as it underestimates $\overline{\rho_v' \rho_v'}$ by 70%. This results in huge values for comparability and bias. The LI-7500 infrared gas analyser shows a good linear relationship when plotted against the reference but its slope deviates from 1.00 the most.

6.5 Friction velocity

Although the Solent-HS was operated in the non-calibrated mode, i.e. without a flow distortion correction, its results for friction velocity u_* are in good agreement with the reference (Table 8). As expected, the agreement of the UW sonic and the two other CSATs is also good. Even the friction velocities measured with the TR90-AH show good agreement, although significant disturbance of the single wind components was detected. The ATI-K probes show larger deviations, and both sensors overestimate u_* by almost 10%. A flow distortion correction factor f of 0.16 instead of 0.20 improves the results only a little. The Metek and R.M. Young sonics do not measure systematically higher or lower u_* values than the reference, but both show a large amount of scatter.

Table 8 Comparison of the friction velocity u_* measurements during EBEX-2000, using CSAT3 (UBT) as reference. Values causing concern are underlined

Sensor	Abs. value a (m s^{-1})	Regression coefficient b	R^2	Comparability $rmsd$ (m s^{-1})	Bias d (m s^{-1})
UW (NCAR)	−0.001	0.97	0.98	0.023	−0.003
CSAT3 (UBS)	−0.009	1.02	0.97	0.025	−0.006
CSAT3 (HK)	0.000	0.99	0.99	0.019	−0.003
Solent-HS (UBS)	−0.005	0.99	0.98	0.022	−0.006
TR90-AH (KNMI/WU)	−0.003	1.00	0.97	0.025	0.003
ATI-K (NCAR) S8[a] $f = 0.16$	−0.010	1.09	0.99	0.020	0.003
ATI-K (NCAR) S8[a] $f = 0.20$	−0.010	1.10	0.98	0.021	0.005
ATI-K (NCAR) S7	−0.008	1.08	0.94	0.030	0.001
USA-1 (UBT)	−0.003	0.99	0.91	0.037	−0.002
R.M. Young (UBT)	0.004	0.98	0.91	0.027	0.002

[a] Here NCAR's UW served as reference instrument, since the Bayreuth CSAT3 was not deployed at the same time as the ATI-K probe at site 8

Table 9 Comparison of the sensible heat flux H measurements during EBEX-2000, using CSAT3 (UBT) as reference. Values causing concern are underlined

Sensor	Abs. value a (W m^{-2})	Regression coefficient b	R^2	Comparability $rmsd$ (W m^{-2})	Bias d (W m^{-2})
UW (NCAR)	−1.5	1.01	0.97	9.3	−1.4
CSAT3 (UBS)	−1.6	0.97	0.99	6.9	−1.7
CSAT3 (HK)	−0.8	0.97	0.98	6.9	−0.9
Solent-HS (UBS)	−2.3	0.97	0.98	8.0	−2.5
TR90-AH (KNMI/WU)	−0.5	1.22	0.99	9.7	2.3
ATI-K (NCAR) S8[a] $f = 0.16$	0.9	1.08	0.98	6.1	0.5
ATI-K (NCAR) S8[a] $f = 0.20$	1.0	1.08	0.98	6.1	0.6
ATI-K (NCAR) S7	0.0	1.00	0.92	8.0	−0.6
USA-1 (UBT)	−1.8	0.83	0.97	12.7	−2.6
R.M. Young (UBT)	−2.8	0.98	0.97	12.8	−3.4

[a] Here NCAR's UW served as reference instrument, since the Bayreuth CSAT3 was not deployed at the same as the ATI-K probe at site 8

6.6 Sensible heat flux

The first four sensors listed in Table 9 show very good agreement with the reference system for estimates of the sensible heat flux H. These are the NCAR UW, the two CSATs from Basel and Hong Kong, and the Solent-HS from Basel, too. The sensible heat fluxes from the R.M. Young sonic are also nearly in the same range as the aforementioned instruments. The Kaijo-Denki sensor overestimates the sensible heat flux, H, whereas the USA-1 underestimates H. The two ATI-K probes behave in different ways. The one at site 8 shows a good correlation but too high a regression coefficient b, whereas the one at site 7 shows a perfect regression line with $a = 0.0$ and $b = 1.0$, but larger scatter. Again, the use of $f = 0.16$ instead of 0.20 leads to a slightly better agreement with the reference.

6.7 Latent heat flux

The values for the latent heat flux λE measured by the UW/KH20 from NCAR are slightly different from those of the reference system CSAT3/KH20 (UBT). Those

Table 10 Comparison of the latent heat flux λE measurements during EBEX-2000, using CSAT3/KH20 (UBT) as reference. Values causing concern are underlined

Sensor complex	Abs. value a (W m^{-2})	Regression coefficient b	R^2	Comparability $rmsd$ (W m^{-2})	Bias d (W m^{-2})
UW/KH20 (NCAR)	−1.9	1.05	0.98	39.0	−9.2
CSAT3/KH20 (HK)	−2.7	0.55	0.97	115.0	−68.6
Solent-HS/KH20 (UBS)	0.9	0.82	0.98	53.3	−26.9
TR90-AH/KH20 (KNMI/WU)	3.7	1.14	0.99	54.0	28.0
CSAT3/LI-7500 (UBT)	−0.7	1.17	1.00	35.7	17.5
ATI-K/KH20 (NCAR)	4.9	0.99	0.95	57.1	3.1

from the other NCAR system ATI-K/KH20 show almost no deviations from the reference. The Solent-HS/KH20 (UBS) underestimates λE even more, and latent heat fluxes measured by the TR90-AH/KH20 (KNMI/WU) are systematically too high. The combination CSAT3/KH20 from Hong Kong measures only approximately half as high evaporation rates as the reference system. The combination of the LI-7500 with the CSAT3 from the University of Bayreuth measures significantly higher λE than the reference combination of the same sonic with a KH20 krypton hygrometer (Table 10).

7 Discussion of sensor characteristics

Looking at Tables 4–6, Tables 8 and 9, which show the parameters measured by sonic anemometers only, we can state that the majority of comparisons have $R^2 > 0.95$ and have a regression coefficient close to 1.00. Of immediate concern are the data from sensors where $R^2 < 0.95$ or a 5% threshold in the slopes of the regression lines is exceeded (regression coefficients 0.95–1.05). These are the wind statistics from the Kaijo-Denki and ATI-K, u_* from the Metek and R.M. Young, and the temperature statistics from the Solent-HS. More problems were found with the humidity measurements of the hygrometers that were tested in the intercomparison.

7.1 Kaijo-Denki TR90-AH/KH20 (KNMI/WU)

The Kaijo-Denki differences are clearly due to inadequate correction for the presence of the krypton hygrometer inside the sonic anemometer array. The problems are especially expressed by $\overline{w'w'}$ values systematically higher than the reference by more than 26% and sensible heat flux measurements that are overestimated by more than 20%. The Kaijo-Denki $\overline{t'_c t'_c}$ variance agrees well with the reference, though with the distorted w, the heat fluxes are too large. Extensive wind-tunnel testing showed that the bulk of the hygrometer severely affected the flow measured by the anemometer. These tests can provide corrections to the data from TR90-AH/KH20 (KNMI/WU). However, as noted above, wind-tunnel-based corrections are generally larger than those encountered in the presence of atmospheric turbulence (Högström and Smedman 2004).

In order to check the wind-tunnel calibration under outdoor turbulent conditions, a comparison between TR90-AH/KH20 sonic/hygrometer configuration and an unobstructed Kaijo-Denki sonic anemometer with 0.20-m pathlength was performed at

Cabauw in The Netherlands. A 20% $\overline{w'w'}$ overshoot was observed, which could be removed after correction with the wind-tunnel calibration. Estimates for the sensible and the latent heat flux were also corrected with this calibration, leading to good agreement with the unobstructed Kaijo-Denki. The friction velocity from the TR90-AH/KH20 already agreed well with the reference before the wind-tunnel calibration. Thus, the findings of Högström and Smedman (2004) regarding the transferability of such corrections to the turbulent atmosphere could not be confirmed. Taking all this into consideration, we decided to add the deviation of 13%, which we found for the standard deviation of the vertical wind speed, as a correction to the sensible heat flux and to the latent heat flux.

7.2 Gill Solent-HS/KH20 (UBS)

The Solent-HS temperature problem has been known for many years, and is manifest in a very high regression coefficient for $\overline{t'_c t'_c}$, a poor correlation and a large *rmsd* value for that parameter; although with the lower $\overline{w'w'}$ (with the internal calibration factor of 1.10 removed), the resulting heat flux is almost acceptable. Several possible reasons for this behaviour in Solent anemometers are discussed by Vogt (1995). The sonic temperature measured by a Solent anemometer shows a significant dependence on the air temperature, due to a temperature dependence of the transducer delay, which results in an erroneous measurement of the speed of sound. Figure 4 shows the temperature dependence of the sonic temperature measurements of the Solent-HS (UBS) and CSAT3 (UBT). The CSAT3 has a dependence on the reference temperature

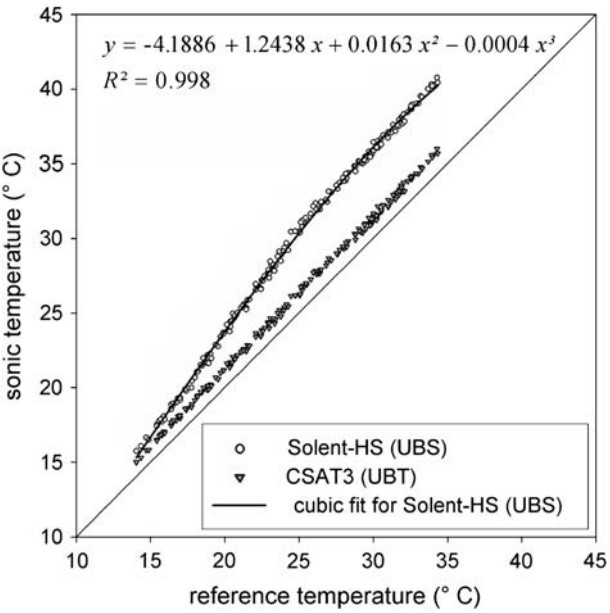

Fig. 4 Sonic temperature measurements of Solent-HS (UBS) and CSAT3 (UBT)) versus reference temperature measured by a psychrometer. The CSAT3 shows a dependency on the reference temperature with a slope close to 1. The relationship between the Solent-HS and the reference temperature can be described by a polynomial fit of third degree: $y = -4.1886 + 1.2438x + 0.0163x^2 - 0.0004x^3$

with a slope close to 1.00. In contrast, the relationship between the Solent-HS sonic temperature $t_{c,\mathrm{solent}}$ and reference temperature T_{ref} from a slow-response ventilated thermometer at the same height can be described by a polynomial fit of third degree:

$$t_{c,\mathrm{solent}} = -0.0004T_{\mathrm{ref}}^3 + 0.0163T_{\mathrm{ref}}^2 + 1.2438T_{\mathrm{ref}} - 4.1886 \quad (4)$$

Equation 4 could be used to correct the raw sonic temperature data of the Solent-HS for the EBEX-2000 experiment period, using the reference air temperature as a proxy for the transducer temperature, which actually caused the changes of the transducer delay.

Not only the sonic anemometer of this sensor combination from the University of Basel showed some problems but also the corresponding krypton hygrometer, which underestimates humidity fluctuations significantly (see Table 7). The behaviour of its sensitivity can be seen in Fig. 5. The difference between the KH20 (UBT) measurement and the psychrometer remains at a near-constant level. Such a constant offset is not relevant for the calculation of variances or covariances, since the average is subtracted. However, the values measured by the KH20 (UBS) not only show a simple offset compared to the reference, their course is completely different from the psychrometer. During the night, this behaviour can be sometimes characterised by a simple offset, but during the day the humidity values of the KH20 (UBS) are relatively lower and have different dynamics than those from the psychrometer. It seems to be an effect of the heating of the sensor's enclosure, beginning after sunrise and proceeding during the day. As mentioned in Sect. 3.2, some components of the KH20 are sensitive to condensation, and we suspect that water condensation in addition to corrosion of electrical contacts produced the misbehaviour of the KH20 from Basel. However, the distinct changes of the KH20's characteristics can hardly be

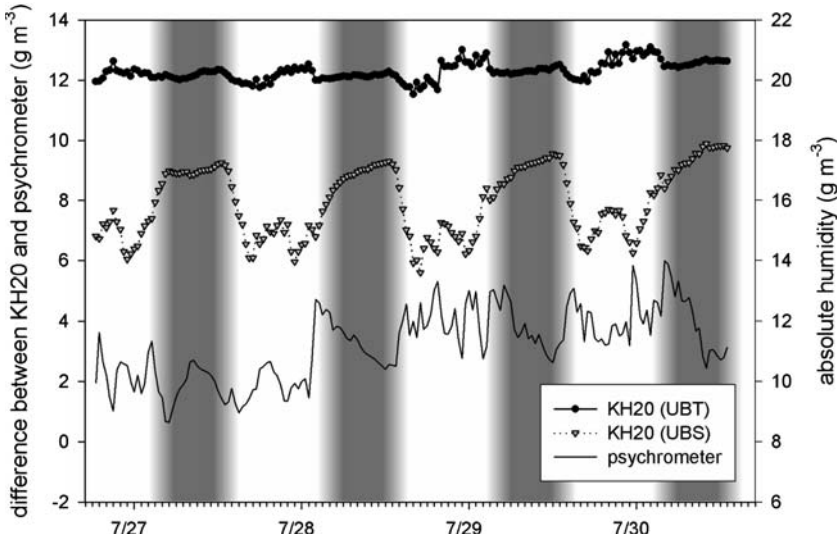

Fig. 5 Differences between the KH20 humidity measurements (UBT and UBS) and the absolute humidity measurement of a reference psychrometer from 1700 UTC, July 26 2000 to 1700 UTC, July 30 2000. All three sensors were deployed at the same height of 4.7 m above ground level. Day/night is indicated by shading of background

reconstructed, and so the latent heat fluxes measured by the Solent-HS/KH20 system were discarded.

7.3 Metek USA-1 and R.M. Young 81000 (UBT)

It is not so obvious why the Metek and R.M. Young exhibit scatter in the u_* comparison. The Metek and R.M. Young wind speeds and $\overline{w'w'}$ differences are larger than 5% (and speed also has a large offset), though the errors compensate accidentally to make u_* comparable. Both of their $\overline{T_s'T_s'}$ values are quite low, though again the higher $\overline{w'w'}$ values make the R.M. Young sensible heat fluxes approximately correct on average. The main problem with the Metek USA-1 is a disturbance of the correlation between the horizontal and the vertical wind components, probably induced by wake effects downstream of a transducer or another supporting structure. According to the theoretical considerations of Wyngaard (1981), probe-induced flow distortion changes the correlation between vertical and horizontal wind components, the so-called crosstalk effect. This is clear in Fig. 6 for the Metek sonic. The CSAT3 has correlation coefficients between w and u that are, as one would expect, almost constant for all wind directions at a value of approximately 0.3. Correlation coefficients measured with the Metek are significantly different from the CSAT3 measurements for certain wind directions, and show a cosine-shape response to wind direction, with a period of approximately 120°. This corresponds to the arrangement of the quite bulky transducer heads.

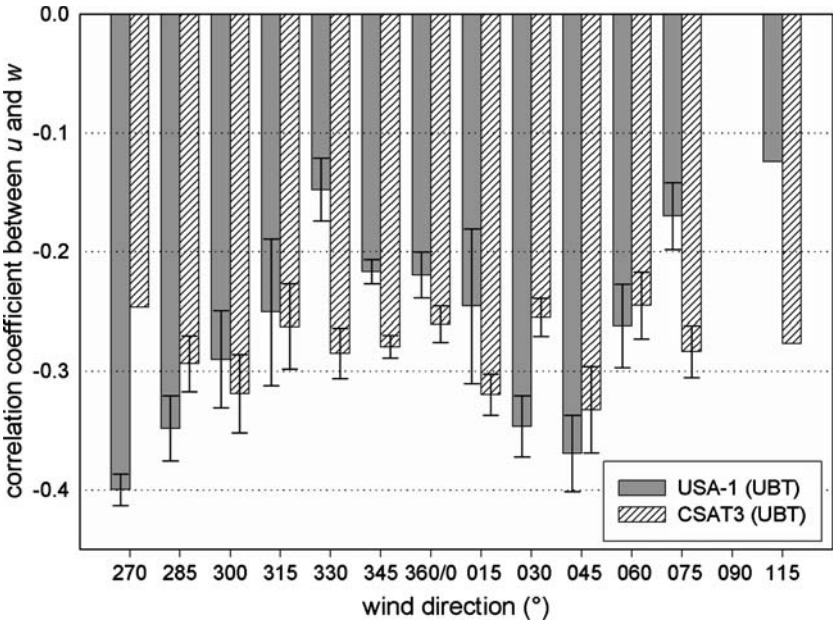

Fig. 6 Correlation coefficients between vertical and horizontal wind velocity depending on wind direction, measured by the CSAT3 (UBT) and the Metek USA-1 (UBT) during EBEX-2000 at site 7. The dataset is subdivided in 15° wind direction classes. Classes of significantly different averages ($\alpha \leq 0.05$) are 330°, 345°, 30°, 75°. Uncertainty ranges are provided for all classes representing more than one value

7.4 ATI-K/KH20 (NCAR)

Based on earlier (unpublished) intercomparison data for the ATI-K probe, which attempted to replicate the study of Kaimal et al. (1990), these had been operated with a single-path correction factor f of 20% maximum (for flow along the path). Significant differences from the reference are obvious in Tables 4, 5 and 8 for the ATI-K probe at site 8 using this correction. Thus, the slightly lower factory default correction of 16% was used to reanalyse these data, which appears to have improved the ATI-K/UW at site 8 comparison slightly. The overestimation of $\overline{w'w'}$ by the ATI-K probe leads to high sensible heat fluxes for this sensor.

For the ATI-K at site 7, high $\overline{w'w'}$ values appear to be balanced by low $\overline{t'_c t'_c}$ values, which results in acceptable sensible heat fluxes. Although the humidity fluctuations are overestimated by the ATI-K/KH20 complex at site 7, its latent heat fluxes also are in good agreement with the reference.

7.5 UW/KH20 (NCAR)

The UW sonic from NCAR generally shows very good agreement with the reference CSAT3 (UBT). For all sonic anemometer test parameters, the slopes of the regression lines are in the range 0.97–1.02 and R^2 values are greater than 0.97. The fact that the UW (NCAR) sensor almost measures the same values as the CSAT3 (UBT) justifies the selection of the latter as the reference instrument. The overall comparison results would not be significantly different if we had chosen the UW (NCAR) instead of the CSAT3 (UBT). The KH20 operating together with the UW sonic also shows good agreement with the reference. The deviations for the parameters $\overline{\rho'_v \rho'_v}$ ($b = 1.06$) and $\lambda E(b = 1.05)$ are slightly larger than those that were measured with only the sonic anemometer, however the scatter is still small ($R^2 \geq 0.98$). Thus, the problem appears to be the calibration of the KH20's sensitivity. This problem could be solved by calibrating the signals from krypton hygrometers to an accurate slow response sensor, which is deployed at the same time and at the same height.

7.6 Campbell CSAT3 (UBS)

Finally, we compare all of the CSAT3s. Differences of up to 4% are seen between the three sensors, and a little larger than one would expect for essentially collocated sensors on a uniform field, but is nevertheless acceptable accuracy for EBEX-2000. The mounting of the CSAT3 (UBS) was different from the reference system, and was fixed to a horizontal tube that was attached to a vertical lattice mast, whereas the remainder of the CSAT3s were fixed to vertical single-tube masts. This can be one reason for the small deviations from the reference that were observed.

7.7 Campbell CSAT3/KH20 (HK)

As mentioned above, the measurements of the CSAT3 from Hong Kong are in very good agreement with the reference, but the variance of humidity measured by the KH20 (HK) is dramatically lower by approximately 70%. Looking at spectra (see Fig. 7) the extinction coefficient for water vapour k_w that is used for the calibration seems to be reasonable, but an attenuation that increases at higher frequencies can be seen. It was not possible to investigate further the reasons for this behaviour. Since the

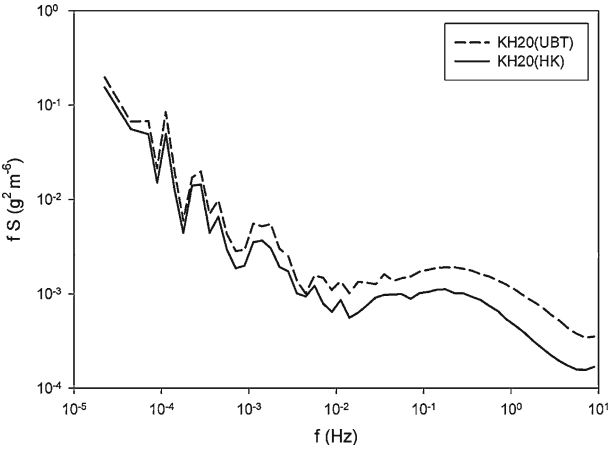

Fig. 7 Spectra of KH20 measurements by the instruments from Bayreuth (reference) and Hong Kong. The signal of the KH20 (HK) is significantly damped compared to the UBT instrument, especially at higher frequencies (dataset: 0300 UTC, July 28 2000 to 0300 UTC, July 29 2000)

R^2 value of 0.97 for the latent heat flux is still high, a correction using the regression coefficients from Table 10 can be considered.

7.8 Campbell CSAT3/LI-7500 (UBT)

The LI-7500 is much better suited for deployment as an absolute instrument than the krypton hygrometer, since it does not suffer from scale on windows and therefore shows no offset compared to a psychrometer. In Fig. 8, the humidity measurements from the LI-7500 (UBT) are shown together with those from a nearby psychrometer. During nighttime, both lines match almost perfectly. But during daytime, the LI-7500 gas analyser measures noticeably higher values than the psychrometer. The difference between both sensors appears to be the largest at noon, when the sun reaches its highest elevation. As this sensor was aligned vertically (see Fig. 3j), it is likely that this phenomenon can be explained by the solar radiation error described above. The excellent correlation ($R^2 = 1.00$) with the reference system allows the use of the regression coefficients from Table 10 in order to obtain comparable results for this sensor combination. Consequently, latent heat fluxes from the combination CSAT3/LI-7500 (UBT) have to be reduced by 17% in general.

One might suspect that differences in the high-frequency response between the KH20 and the LI-7500 are the reason for the discrepancies between both sensor types. These could either be due to the different pathlength or different separation between the hygrometer and the sonic or to a different frequency response of the hygrometers. The first two effects were corrected through the Moore correction, whereas the separation was also very similar. The KH20 shows some aliasing in the high-frequency part of the spectra (Fig. 7); however, this effect should have no impact on variances or on covariances, since the spectral energy is conserved, and is only represented at different frequencies in the spectrum (Horst 2000). The LI-7500 has an internal anti-aliasing filter, and so in this case spectral energy from frequencies higher than the cut-off frequency is not captured. However, this lost energy should be small

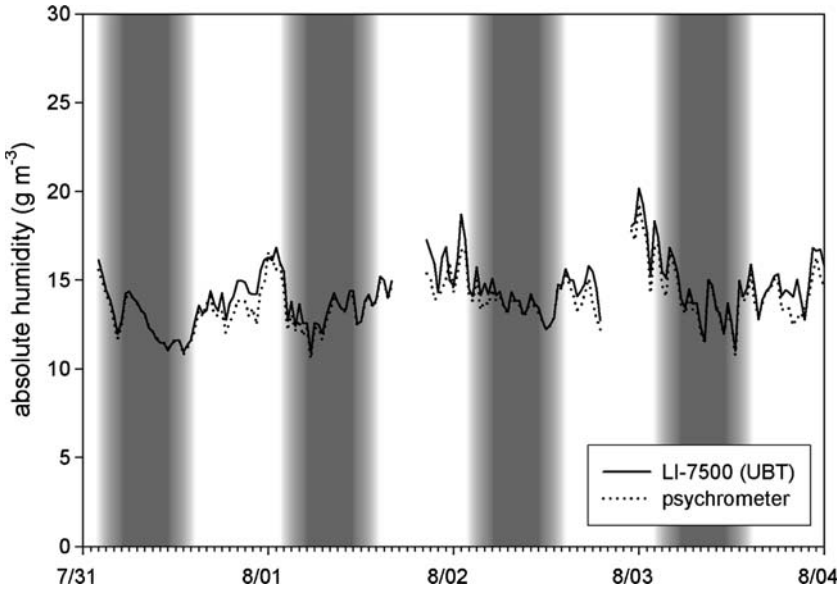

Fig. 8 Absolute humidities ($g\,m^{-3}$) measured by the LI-7500 (UBT) and a psychrometer from 0000 UTC, July 31 2000 to 0000 UTC, August 4 2000, both deployed at the same height of 4.7 m above ground level. Note the changing calibration of LI-7500 (UBT) infrared gas analyser, especially the differences between daytime and nighttime. Day/night is indicated by shading of background

and most probably does not explain the discrepancies between the LI-7500 and the KH20s.

8 Conclusions

In order to achieve good eddy-covariance sensor intercomparison results, it is important to standardise the mounting of the sensors, data acquisition, data processing and calibration of hygrometers as much as possible. We found excellent agreement between the CSAT3/KH20 (UBT) and the UW/KH20 (NCAR) for all test parameters and also with the other CSATs for the parameters measured by a sonic anemometer only. This justifies the choice of the former as the reference for this comparison study, although the results would not be much different if one had chosen the latter.

Most of the eddy-covariance systems showed good agreement for heat flux measurements, especially those from NCAR, which were predominantly used at the ten sites at EBEX-2000. For the remainder of the systems, wherever we found major deviations, possible reasons for their misbehaviour were analysed and suggestions for correcting these measurements were made. No dependence of the intercomparison results on the distance of the single systems to the reference system could be identified.

From this study, the UW and CSAT3 sonics can be classified as well-qualified instruments suitable for fundamental research on turbulence if operated properly. Some minor deficiencies were found for the Solent-HS and the ATI-K probes. The Metek USA-1 and the R.M. Young showed larger problems regarding flow distortion and crosstalk due to transducer-shadow effects. Nevertheless, these sensors can be used for general turbulent flux measurements.

Sonic anemometers can be used for absolute measurements of wind velocities. Well-calibrated krypton hygrometers are suitable for relative measurements of turbulent humidity fluctuations but cannot serve as absolute instruments for humidity because of large offsets due to scale accumulation on the optical windows. To reduce these unwanted effects, daily cleaning of the windows is necessary and great attention has to be attached to the calibration of these sensors.

The LI-7500 open path gas analyser, which we used during EBEX-2000, suffered some "teething troubles" (it was one of the first serial numbers). Now that these problems of solar radiation error and delay time error have been solved by the manufacturer, we expect that this instrument type is satisfactory for the eddy-covariance measurement of latent heat flux.

The comparison of post-field data processing methods showed that typical differences in methodologies can result in discrepancies of up to 15% for the sensible and latent heat flux. A proper correction for spatial separation of sensors was found to be very important. Linear detrending can also have a large impact on the resulting flux, since it acts as a high-pass filter for longwave flux contributions. In general, only minor differences were found between different methods due to discrepancies in the order of processing steps and the use of physical constants.

Neither the errors due to different eddy covariance post-field data processing methods nor the errors due to instrumental deficiencies were found to be systematic in such a way that they can explain the energy balance closure problem in general, because most of the errors found are too small or do not affect turbulent fluxes in the right direction. However, some discrepancies related to the operation of turbulence instruments have been exposed. Furthermore, the discussion of methodological aspects of the eddy-covariance data analysis has led to a better definition of a uniform processing algorithm.

Acknowledgements Each participant in EBEX-2000 has been funded primarily through his or her own institution and some contributed personal resources. Funding for the deployment of NCAR facilities was provided by the National Science Foundation. Heping Liu's contribution was partly supported by City University of Hong Kong (Grant 8780046 and SRG 7001038). Arrangement for use of the field site was facilitated by Bruce Roberts, Director of the University of California Cooperative Extension, Kings County. Westlake Farms generously provided both use of the land for this experiment and helped with logistical support. We are grateful to all of these people and organisations.

References

Aubinet M, Grelle A, Ibrom A, Rannik Ü, Moncrieff J, Foken T, Kowalski AS, Martin PH, Berbigier P, Bernhofer C, Clement R, Elbers J, Granier A, Grünwald T, Morgenstern K, Pilegaard K, Rebmann C, Snijders W, Valentini R, Vesala T (2000) Estimates of the annual net carbon and water exchange of forests: The EUROFLUX methodology. Adv Ecol Res 30:113–175

Beyrich F, Richter SH, Weisensee U, Kohsiek W, Lohse H, DeBruin HAR, Foken T, Göckede M, Berger FH, Vogt R, Batchvarova E (2002) Experimental determination of turbulent fluxes over the heterogeneous LITFASS area: Selected results from the LITFASS-98 experiment. Theor Appl Climatol 73:19–34.

Brook RR (1978) The influence of water vapor fluctuations on turbulent fluxes. Boundary-Layer Meteorol 15:481–487

Businger JA, Dabberdt WF, Delany AC, Horst TW, Martin CL, Oncley SP, Semmer SR (1990) The NCAR atmospheric-surface turbulent exchange research (ASTER) facility. Bull Amer Meteorol Soc 71:1004–1011

Christen A, van Gorsel E, Andretta M, Calanca M, Rotach M, Vogt R (2000) Intercomparison of ultrasonic anemometers during the MAP-Riviera project. In: 9th Conference on Mountain Meteorology, Aspen, CO, pp 130–131

Culf AD, Foken T, Gash JHC (2004) The energy balance closure problem. In: Kabat P, Claussen M (eds) Vegetation, water, humans and the climate. A New Perspective on an Interactive System, Springer, Berlin, Heidelberg, pp 159–166

Dyer AJ (1981) Flow distortion by supporting structures. Boundary-Layer Meteorol 20:363–372

Dyer AJ, Garratt JR, Francey RJ, McIlroy IC, Bacon NE, Bradley EF, Denmead OT, Tsvang LR, Volkov YA, Koprov BM, Elagina LG, Sahashi K, Monji N, Hanafusa T, Tsukamoto O, Frenzen P, Hicks BB, Wesely M, Miyake M, Shaw W (1982) An international turbulence comparison experiment (ITCE-76). Boundary-Layer Meteorol 24:181–209

Finnigan JJ, Clement R, Malhi Y, Leuning R, Cleugh HA (2003) A re-evaluation of long-term flux measurement techniques, Part I: averaging and coordinate rotation. Boundary-Layer Meteorol 107:1–48

Foken T, Skeib G, Richter SH (1991) Dependence of the integral turbulence characteristics on the stability of stratification and their use for Doppler-Sodar measurements. Z. Meteorol 41:311–315

Foken T, Oncley SP (1995) Workshop on instrumental and methodical problems of land surface flux measurements. Bull Amer Meteorol Soc 76:1191–1193

Foken T, Wichura B (1996) Tools for quality assessment of surface-based flux measurements. Agric For Meteorol 78:83–105

Foken T, Weisensee U, Kirzel H-J, Thiermann V (1997) Comparison of new-type sonic anemometers. In: 12th Symposium on Boundary Layer and Turbulence. Vancouver, BC, Amer. Meteorol. Soc., Boston, pp 356–357

Foken T (1998) Die scheinbar ungeschlossene Energiebilanz am Erdboden—eine Herausforderung an die Experimentelle Meteorologie. Sitzungsberichte der Leibniz-Sozietät 24:131–150

Foken T (1999) Comparison of the sonic anemometer Young Model 81000 during VOITEX-99. Universität Bayreuth, Abt. Mikrometeorologie, Arbeitsergebnisse vol 8, 12 pp (Print, ISSN 1614–8916; Internet, ISSN 1614–8926)

Foken T, Göckede M, Mauder M, Mahrt L, Amiro BD, Munger JW (2004) Post-field data quality control. In: Lee X, Massman WJ, Law BE (eds) Handbook of micrometeorology. A guide for surface flux measurements. Kluwer, Dordrecht, pp 181–208

Högström U, Smedman A-S (2004) Accuracy of sonic anemometers: laminar wind-tunnel calibrations compared to atmospheric in situ calibrations against a reference instrument. Boundary-Layer Meteorol 111:33–54

Højstrup J (1993) A statistical data screening procedure. Meas Sci Technol 4:153–157

Horst TW (2000) On frequency response corrections for eddy covariance flux measurements. Boundary-Layer Meteorol 94:517–520

ISO (1993) Statistics—vocabulary and symbols—Part 1: probability and general statistical terms. International Organization for Standardization, Geneva, Switzerland, ISO 3534–1, 61 pp

Jegede OO, Foken T (1999) A study of the internal boundary layer due to a roughness change in neutral conditions observed during the LINEX field campaigns. Theor Appl Climatol 62:31–41

Kaimal JC, Gaynor JE, Zimmerman HA, Zimmerman GA (1990) Minimizing flow distortion errors in a sonic anemometer. Boundary-Layer Meteorol 53:103–115

Kaimal JC, Finnigan JJ (1994) Atmospheric boundary layer flows their structure and measurement. Oxford university press, New York, NY, 289 pp

Laubach J, Teichmann U (1996) Measuring energy budget components by eddy correlation: data corrections and application over low vegetation. Contr Atmos Phys 69:307–320

Lee X, Massman W, Law BE (eds) (2004) Handbook of micrometeorology. A guide for surface flux measurement and analysis. Kluwer Academic Press, Dordrecht, 250 pp

Liu H, Peters G, Foken T (2001) New equations for sonic temperature variance and buoyancy heat flux with an omnidirectional sonic anemometer. Boundary-Layer Meteorol 100:459–468

Mauder M, Foken T (2004) Documentation and instruction manual of the eddy covariance software package TK2. Universität Bayreuth, Abt. Mikrometeorologie, Arbeitsergebnisse vol 26, 44 pp (Print: ISSN 1614–8916; Internet: ISSN 1614–8926)

Mestayer PG, Durand P, Augustin P, Bastin S, Bonnefond J-M, Bénech B, Campistron B, Coppalle A, Delbarre H, Dousset B, Drobinski P, Druilhet A, Fréjafon E, Grimmond CSB, Groleau D, Irvine M, Kergomard C, Kermadi S, Lagouarde J-P, Lemonsu A, Lohou F, Long N, Masson V, Moppert C, Noilhan J, Offerle B, Oke TR, Pigeon G, Puygrenier V, Roberts S, Rosant J-M, Sanid F, Salmond J, Talbaut M, Voogt J (2005) The urban boundary-layer field campaign in marseille (ubl/clu-escompte): set-up and first results. Boundary-Layer Meteorol 114:315–365

Miyake M, Stewart RW, Burling HW, Tsvang LR, Koprov BM, Kuznetsov OA (1971) Comparison of acoustic instruments in an atmospheric turbulent flow over water. Boundary-Layer Meteorol 2:228–245

Mölder M, Klemedtsson L, Lindroth A (2004) Turbulence characteristics and dispersion in a forest—tests of Thomson's random-flight model. Agric For Meteorol 127:203–222

Moore CJ (1986) Frequency response corrections for eddy correlation systems. Boundary-Layer Meteorol 37:17–35

Oncley SP, Foken T, Vogt R, Bernhofer C, Kohsiek W, Liu H, Pitacco A, Grantz D, Ribeiro L, Weidinger T (2002) The energy balance experiment EBEX-2000. In: 15th Symposium on Boundary Layer and Turbulence. Wageningen, NL, Am Meteorol Soc, 1–4

Oncley SP, Foken T, Vogt R, Kohsiek W, de Bruin H, Bernhofer C, Christen A, Grantz D, Lehner E, Liebethal C, Liu H, Mauder M, Pitacco A, Ribeiro L, Weidinger T (2007) The energy balance experiment EBEX-2000. Part I: overview and energy balance. Boundary-Layer Meteorol (in press)

Schotanus P, Nieuwstadt FTM, DeBruin HAR (1983) Temperature measurement with a sonic anemometer and its application to heat and moisture fluctuations. Boundary-Layer Meteorol 26:81–93

Tanner BD, Campbell GS (1985) A krypton hygrometer for measurement of atmospheric water vapor concentration. In: Moisture and humidity. Instrument Society of America, Research Triangle Park, NC, pp 609–612

Tanner BD, Swiatek E, Greene JP (1993) Density fluctuations and use of the krypton hygrometer in surface flux measurements. In: Allen RG (ed) Management of irrigation and drainage systems: integrated perspectives. American Society of Civil Engineers, New York, NY, pp 945–952

Thomas C, Foken T (2002) Re-evaluation of integral turbulence characteristics and their parameterisations. In: 15th Conference on Turbulence and Boundary Layers, Wageningen, NL, Am Meteorol Soc, pp 129–132

Tsvang LR, Koprov BM, Zubkovskii SL, Dyer AJ, Hicks B, Miyake M, Stewart RW, McDonald JW (1973) A comparison of turbulence measurements by different instruments; Tsimlyansk field experiment 1970. Boundary-Layer Meteorol 3:499–521

Tsvang LR, Zubkovskij SL, Kader BA, Kallistratova MA, Foken T, Gerstmann W, Przandka Z, Pretel J, Zelený J, Keder J (1985) International turbulence comparison experiment (ITCE-81). Boundary-Layer Meteorol 31:325–348

van Dijk A, Kohsiek W, DeBruin HAR (2003) Oxygen sensitivity of krypton and Lyman-alpha hygrometers. J Atmos Oceanic Tech 20:143–151

Vogt R (1995) Theorie, Technik und Analyse der experimentellen Flussbestimmung am Beispiel des Hartheimer Kiefernwaldes. University of Basel, Basel, Switzerland, Stratus vol 3, 101 pp

Webb EK, Pearman GI, Leuning R (1980) Correction of the flux measurements for density effects due to heat and water vapour transfer. Quart J Roy Meteorol Soc 106:85–100

Webb EK (1982) On the correction of flux measurements for effects of heat and water vapour transfer. Boundary-Layer Meteorol 23:251–254

Wilczak JM, Oncley SP, Stage SA (2001) Sonic anemometer tilt correction algorithms. Boundary-Layer Meteorol 99:127–150

Wilson K, Goldstein A, Falge E, Aubinet M, Baldocchi D, Berbigier P, Bernhofer C, Ceulemans R, Dolman H, Field C (2002) Energy balance closure at FLUXNET sites. Agric For Meteorol 113:223–243

Wyngaard JC (1981) The effects of probe-induced flow distortion on atmospheric turbulence measurements. J Appl Meteorol 20:784–794

Wyngaard JC, Zhang SF (1985) Transducer-shadow effects on turbulence spectra measured by sonic anemometers. J Atmos Oceanic Tech 2:548–558

Zhang SF, Wyngaard JC, Businger JA, Oncley SP (1986) Response characteristics of the U.W. sonic anemometer. J Atmos Oceanic Tech 2:548–558